



Mixed formulation for an easy and robust numerical computation of sorptivity

Laurent Lassabatere¹, Pierre-Emmanuel Peyneau², Deniz Yilmaz³, Joseph Pollacco⁴,
Jesús Fernández-Gálvez⁵, Borja Latorre⁶, David Moret-Fernández⁶, Simone Di Prima⁷,
Mehdi Rahmati^{8,9}, Ryan D. Stewart¹⁰, Majdi Abou Najm¹¹, Claude Hammecker¹², and
Rafael Angulo-Jaramillo¹

¹Univ Lyon, Université Claude Bernard Lyon 1, CNRS, ENTPE, UMR5023 LEHNA, F-69518, Vaulx-en-Velin, France

²GERS-LEE, Univ Gustave Eiffel, IFSTTAR, F-44344 Bouguenais, France

³Civil Engineering Department, Engineering Faculty, Munzur University, Tunceli, Turkey

⁴Manaaki Whenua - Landcare Research, 7640 Lincoln, New Zealand

⁵Department of Regional Geographic Analysis and Physical Geography, University of Granada, 18071 Granada, Spain

⁶Departamento de Suelo y Agua, Estación Experimental de Aula Dei, Consejo Superior de Investigaciones Científicas (CSIC), PO Box 13034, 50080 Zaragoza, Spain

⁷Agricultural Department, University of Sassari, Viale Italia, 39, 07100 Sassari, Italy

⁸Department of Soil Science and Engineering, Faculty of Agriculture, University of Maragheh, Maragheh, Iran

⁹Forschungszentrum Jülich GmbH, Institute of Bio- and Geosciences: Agrosphere (IBG-3), Jülich, Germany

¹⁰School of Plant and Environmental Sciences, Virginia Polytechnic Institute and State University, Blacksburg, VA, United States

¹¹Department of Land, Air and Water Resources, University of California, Davis, CA 95616, United States

¹²University of Montpellier, UMR LISAH, IRD, Montpellier, France

Correspondence: Laurent Lassabatere (laurent.lassabatere@entpe.fr)

Abstract.

Sorptivity is one of the most important parameters for the quantification of water infiltration into soils. Parlange (1975) proposed a specific formulation to derive sorptivity as a function of the soil water retention and hydraulic conductivity functions, as well as initial and final soil water contents. However, this formulation requires the integration of a function involving the hydraulic diffusivity, which may be undefined or present numerical difficulties that cause numerical misestimations. In this study, we propose a mixed formulation that scales sorptivity and splits the integrals into two parts: the first term involves the scaled degree of saturation while the second involves the scaled water pressure head. The new mixed formulation is shown to be robust and well-suited to any type of hydraulic functions - even with infinite hydraulic diffusivity or positive air-entry water pressure heads - and any boundary condition, including infinite initial water pressure head, $h \rightarrow -\infty$.

10 1 Introduction

Soil sorptivity represents the capacity of a soil to absorb or desorb liquid by capillarity, and is therefore one of the key factors for modeling water infiltration into soil or flow in the vadose zone (Cook and Minasny, 2011). Knowledge of soil sorptivity is also crucial when deciphering soil physical properties such as hydraulic conductivity from water infiltration experiments



(Angulo-Jaramillo et al., 2016; Stewart and Abou Najm, 2018). Several models and methods make use of this variable such as in the the Beerkan Estimation of Soil Transfer parameters (BEST) methods (Lassabatere et al., 2006, 2009, 2014, 2019; Angulo-Jaramillo et al., 2019) and related simplified Beerkan approaches (Bagarello et al., 2014b; Di Prima et al., 2020; Yilmaz, 2021). Sorptivity is also required for the computation of several hydraulic parameters, like the macroscopic capillary length (Bouwer, 1964; White and Sully, 1987). Parlange (1975) proposed an accurate approximation for the quantification of sorptivity:

$$S_D(\theta_0, \theta_1) = \sqrt{\int_{\theta_0}^{\theta_1} (\theta_1 + \theta - 2\theta_0) D(\theta) d\theta} \quad (1)$$

where $D(\theta) = K(\theta)dh/d\theta$ is the hydraulic diffusivity function, θ_0 and θ_1 stand for the initial and final water contents. This formulation addresses the case when the initial and final conditions are defined in terms of water contents. Ross et al. (1996) defined this integral in terms of water pressure head instead of water contents, leading to the following formulation:

$$\begin{aligned} S_K(h_0, h_1) &= \sqrt{\int_{h_0}^{h_1} (\theta(h_1) + \theta(h) - 2\theta(h_0)) K(h) dh} \\ &= \sqrt{\int_{h_0}^{h_1} (\theta_1 + \theta(h) - 2\theta_0) K(h) dh} \end{aligned} \quad (2)$$

where the initial and the final values of the water pressure heads, h_0 and h_1 , correspond to the water contents $\theta_0 = \theta(h_0)$ and $\theta_1 = \theta(h_1)$. In the following, the two equations Eq. (1) and Eq. (2) will be referred to as the diffusivity and conductivity forms of sorptivity and will be respectively denoted S_D and S_K .

The two forms, S_K and S_D , each have their own shortcomings. For certain hydraulic models, $D(\theta)$ tends towards infinity when $\theta_0 \rightarrow \theta_s$, making it difficult to compute the right-hand side of Eq. (1). Moreover, when the surface water pressure head exceeds the air-entry water pressure head, S_D misses the saturated part of sorptivity, $\int_{h_a}^{h_1} (\theta(h_1) + \theta(h) - 2\theta(h_0)) K(h) dh$ (Ross et al., 1996). The conductivity form S_K must be used when it is necessary to account for the two parts of sorptivity, i.e., the unsaturated and saturated parts, as indicated by the following relationship (Lassabatere et al., 2021):

$$\begin{aligned} S_K(h_0, h_1 \geq h_a) &= \sqrt{S_D^2(\theta_0, \theta_s) + 2(\theta_s - \theta_0) K_s(h_1 - h_a)} \\ &= \sqrt{S_D^2(\theta(h_0), \theta(h_1)) + 2(\theta(h_1) - \theta(h_0)) K_s(h_1 - h_a)} \end{aligned} \quad (3)$$

We can thus conclude that the conductivity form, S_K , is the more general equation. However, S_K can also be difficult to handle when the initial conditions are very dry. In particular, for very dry initial conditions, the initial water pressure head corresponding to θ_r corresponds to $h_0 \rightarrow -\infty$. Then, the calculation of S_K requires the evaluation of an integral that involves an infinite lower bound: $\int_{-\infty}^{h_1} (\theta(h_1) + \theta(h) - 2\theta_r) K(h) dh$.

In this study, we propose a new mixed formulation that overcomes these problems. We compare it to the approaches commonly used to compute sorptivity, i.e., Eq. (1) and Eq. (2). The proposed mixed formulation automatically accounts for the



40 saturated and unsaturated parts of sorptivity. It also allows for easy computation under any initial condition, including the extreme case of an initial water content equal to the residual water content, $\theta_0 = \theta_r$ (corresponding to a negative infinite initial water pressure head, $h_0 = -\infty$) and a final water pressure head higher than the air-entry water pressure head, $h_1 \geq h_a$.

The paper is organized as follows. The theory section presents the proposed mixed formulation. Next, the paper analyzes the precision of the mixed formulation by comparing it with the exact analytical formulation for the case of the maximum
 45 sorptivity, $S(-\infty, 0) = \sqrt{\int_{-\infty}^0 (\theta_s + \theta(h) - 2\theta_r) K(h) dh}$. The maximum sorptivity, $S(-\infty, 0)$, encompasses the two types of problems, i.e., infinite negative initial water pressure head, and infinite diffusivity function close to water saturation $\theta \rightarrow \theta_s$, and also omission of the saturated part of sorptivity when $h_1 > h_a$ by regular approaches. We considered three commonly used hydraulic models, for which Lassabatere et al. (2021) proposed analytical formulations for $S(-\infty, 0)$: Brooks and Corey (BC), van Genuchten - Burdine (vGB), and van Genuchten - Mualem (vGM). See below for their descriptions. The second part
 50 of the paper compares the accuracy of the mixed formulation with the current strategies for the same three hydraulic models plus the Kosugi (KG) model, that demonstrating the risk of serious misestimations with prior approaches. By presenting a new formulation that is applicable to any types of conditions, this paper completes the study of Lassabatere et al. (2021), who proposed a scaling procedure for the approximation of $S_K(h_0, h_1 = 0)$ with the condition of null water pressure head at surface, i.e., $h_1 = 0$.

55 2 Theory

2.1 Proposed new mixed formulation for computing sorptivity

To build the mixed formulation, S_M , we start with the conductivity form of sorptivity, S_K , since it includes both unsaturated and saturated parts. Then, we define an intermediate water pressure head between the initial and final water pressure heads, $h_c \in [h_0, h_1]$, smaller than the air entry pressure, $h_c < h_a \leq 0$, and we split the integrate into two separate parts as follows:

$$\begin{aligned}
 S_M(h_0, h_1) &= S_K(h_0, h_1) = \sqrt{\int_{h_0}^{h_1} (\theta(h_1) + \theta(h) - 2\theta(h_0)) K(h) dh} \\
 &= \sqrt{\int_{h_0}^{h_c} (\theta(h_1) + \theta(h) - 2\theta(h_0)) K(h) dh + \int_{h_c}^{h_1} (\theta(h_1) + \theta(h) - 2\theta(h_0)) K(h) dh} \\
 60 \quad &= \sqrt{\int_{\theta(h_0)}^{\theta(h_c)} (\theta(h_1) + \theta - 2\theta(h_0)) D(\theta) d\theta + \int_{h_c}^{h_1} (\theta(h_1) + \theta(h) - 2\theta(h_0)) K(h) dh} \quad (4)
 \end{aligned}$$

In Eq. (4), the integral $\int_{h_0}^{h_c} (\theta(h_1) + \theta(h) - 2\theta(h_0)) K(h) dh$ is transformed into $\int_{\theta(h_0)}^{\theta(h_c)} (\theta(h_1) + \theta - 2\theta(h_0)) D(\theta) d\theta$ thanks to the change of variable $h \rightarrow \theta$. This operation requires that the function $\theta(h)$ is bijective over the whole interval $[h_0, h_c]$,



which is valid so long as $h_c < h_a$. The mixed formulation, S_M , may be written alternatively as follows:

$$S_M(h_0, h_1) = \sqrt{\underbrace{\int_{\theta_0}^{\theta_c} (\theta_1 + \theta - 2\theta_0) D(\theta) d\theta}_A + \underbrace{\int_{h_c}^{h_1} (\theta_1 + \theta(h) - 2\theta_0) K(h) dh}_B} \quad (5)$$

65 where $\theta_c = \theta(h_c)$ and $\theta_1 = \theta(h_1)$ and $\theta_0 = \theta(h_0)$. The constraint $h_c < h_a$ ensures that the computation of A in Eq. (5) avoids the challenging integration of infinite diffusivity close to saturation, $D(\theta_s) = +\infty$, since $\theta_c < \theta_s$. In addition, h_c is bounded to finite value to avoid integration over infinite intervals for part B. Then, the two integrals involved in Eq. (5), A and B only involve bounded functions over finite intervals, ensuring an easy numerical computation. An illustration of the procedure is depicted in Figure (1).

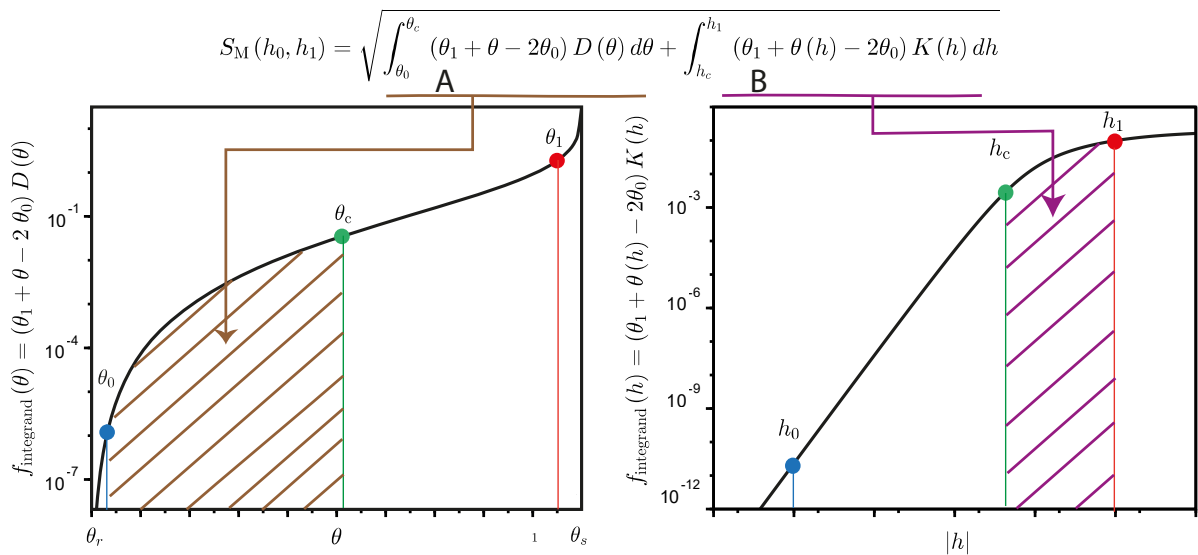


Figure 1. Concept of the mixed formulation, $S_M(h_0, h_1)$: the integration of $\int_{h_0}^{h_1} (\theta_1 + \theta(h) - 2\theta_0) K(h) dh$ ($= S_M^2(h_0, h_1)$) is converted into the sum of the integration of two bounded functions over bounded intervals, $\int_{\theta_0}^{\theta_c} (\theta_1 + \theta - 2\theta_0) D(\theta) d\theta$ and $\int_{h_c}^{h_1} (\theta_1 + \theta(h) - 2\theta_0) K(h) dh$. Note that the data are depicted with log-scale for clarity but the integration performs on directly on the integrands instead of their log-scaled counterparts.

70 Next, we scale sorptivity to separate the respective contributions of scale and shape parameters, as suggested by Lassabatere et al. (2021). We consider the following scaling relationships for hydraulic variables and sorptivity:

$$\begin{cases} S_e = \frac{\theta - \theta_r}{\theta_s - \theta_r} \\ h^* = \frac{h}{|h_g|} \\ K_r = \frac{K}{K_s} \end{cases} \quad (6)$$



where S_e is the saturation degree, h^* is the scaled water pressure head, K_r is the relative hydraulic conductivity, θ_r and θ_s are the residual and the saturated water contents, h_g is the scale parameter for the water pressure head, and K_s is the saturated hydraulic conductivity. The application of scaling relationships of Eq. (6) to the dimensional sorptivity expressions leads to the following equation (Ross et al., 1996):

$$S = \sqrt{|h_g| K_s (\theta_s - \theta_r)} S^* \quad (7)$$

where S and S^* are respectively the dimensional and the scaled sorptivities. The application of the scaling equations Eqs. (6-7) to the mixed formulation S_M , defined by Eq. (4), leads to the final expression proposed in this study:

$$80 \quad \begin{cases} S_M(h_0, h_1) = \sqrt{|h_g| K_s (\theta_s - \theta_r)} S_M^*(h_0^*, h_1^*) \\ S_M^*(h_0^*, h_1^*) = \sqrt{\int_{S_e(h_0^*)}^{S_e(h_1^*)} (S_e(h_1^*) + S_e - 2S_e(h_0^*)) D^*(S_e) dS_e + \int_{h_c^*}^{h_1^*} (S_e(h_1^*) + S_e(h^*) - 2S_e(h_0^*)) K_r(h^*) dh^*} \end{cases} \quad (8)$$

where $S_M^*(h_0^*, h_1^*)$ is the scaled version of the proposed mixed formulation, $S_M(h_0, h_1)$, with $h_0^* = h_0/|h_g|$ and $h_1^* = h_1/|h_g|$. Eq. (8) can be demonstrated by changing the integration variable $\theta \rightarrow S_e$ in the first and $h \rightarrow h^*$ in the second integral of Eq. (4). The equation Eq. (8) has an inconvenient with coding software that do not allow infinite value, $h_0^* = -\infty$. We then replace the input h_0 (that may be infinite) with $S_{e,0} = S_e(h_0^*)$ that always remains bounded in the final expression of the mixed formulation S_M^* :

$$85 \quad S_M^*(S_{e,0}, h_1^*) = \sqrt{\int_{S_{e,0}}^{S_e(h_c^*)} (S_e(h_1^*) + S_e - 2S_{e,0}) D^*(S_e) dS_e + \int_{h_c^*}^{h_1^*} (S_e(h_1^*) + S_e(h^*) - 2S_{e,0}) K_r(h^*) dh^*} \quad (9)$$

Several options exist for the choice of the intermediate water pressure head h_c^* and intermediate saturation degree $S_{e,c} = S_e(h_c^*)$. In this study, our preferred option is to set the intermediate saturation degree as the average between the initial and the final saturation degrees, $S_{e,c} = (S_{e,0} + S_{e,1})/2$. However, under certain circumstances (e.g., for soils with gradual water retention functions, see results section), the value of $h^*(S_{e,c})$ may reach very large values, leading to numerical instabilities. Therefore, we use the following criteria to ensure that $h^*(S_{e,c})$ remains finite:

$$95 \quad \begin{cases} h_c^* = -\min\left(\left|h^*\left(\frac{S_{e,0} + S_{e,1}}{2}\right)\right|, 10^z\right) \quad z \in \mathbb{Z} \\ S_{e,c} = S_e(h_c^*) \end{cases} \quad (10)$$

When necessary, the value of z is varied until the two integrals in S_M^* (Eq. 9) converge. In most cases, $z \in \{-2, -1, 0\}$ ensures convergence regardless of soil type and situation. Note that for hydraulic models with non-null water entry pressure head $h_a < 0$, z should be fixed with $z \geq 0$ so as to ensure $-10^z \leq -1$ and thus $h_c^* \leq h_a^* = -1$. This condition is necessary to ensure the bijectivity of the function $S_e(h^*)$ over the interval $[h_0^*, h_c^*]$, which is required for the use of Eq. (9).

In the following, the mixed formulation S_M^* , Eqs. (9-10) will be compared to several strategies previously proposed in the literature to cope with situations of numerical indeterminacy, e.g., at saturation $\theta_1 = \theta_s$ (or, $S_{e,1} = 1$) for a null water pressure head at surface, $h_1 = 0$, and for very dry initial conditions $\theta_0 \rightarrow \theta_r$ (or, $h_0^* \rightarrow -\infty$).



100 **2.2 Usual methods for computing sorptivity based on S_D and S_K**

2.2.1 Computing sorptivity with S_K for very dry initial conditions $h_0 \rightarrow -\infty$

Regarding the computation of sorptivity for very dry initial conditions with S_K , one of the strategies found in the literature applies the regular definitions of sorptivity (Parlange, 1975), Eq. (2), to the case of very low values of h_0 . Such an approach was used by Di Prima et al. (2020) for the estimation of $S_K(h_0, h_1)$ for very dry soils. In this case, the maximum sorptivity,

105 $S(-\infty, h_1)$, is approached as follows:

$$\begin{aligned}
 S(-\infty, h_1) &= \sqrt{\int_{-\infty}^{h_1} (\theta_1 + \theta(h) - 2\theta_r) K(h) dh} \\
 &= \lim_{h_0 \rightarrow -\infty} \sqrt{\int_{\underline{h_0}}^{h_1} (\theta_1 + \theta(h) - 2\underline{\theta(h_0)}) K(h) dh} \\
 &= \lim_{h_0 \rightarrow -\infty} S_K(\underline{h_0}, h_1)
 \end{aligned} \tag{11}$$

Note that, for the sake of clarity, the underline in Eq. (11) shows the variables that are varied. Note also that the preceding equations are valid since $\sqrt{\lim f(x)} = \lim \sqrt{f(x)}$, with $y = \sqrt{x}$ defining a continuous function. In practical applications of this method, $S_K(h_0, h_1)$ is computed for decreasing values of h_0 until reaching stabilization, since the integration can lead to numerical indeterminacy when the intervals $[h_0, h_1]$ are too wide. The last value obtained in this way is considered to represent the sorptivity at extremely dry conditions, i.e., $S(-\infty, h_1)$. This option is quite practical since it requires the user to only code the regular function S_K before applying it to very negative values of h_0 .

110

We propose an alternative procedure that employs a specific integrand to compute the same limit. In this case, the water content θ_0 is set equal to θ_r in the integrand so as to correspond to the targeted initial conditions $\theta(h_0 = -\infty) = \theta_r$:

$$\begin{aligned}
 S(-\infty, h_1) &= \sqrt{\int_{-\infty}^{h_1} (\theta_1 + \theta(h) - 2\theta_r) K(h) dh} \\
 &= \lim_{h_0 \rightarrow -\infty} \sqrt{\int_{\underline{h_0}}^{h_1} (\theta_1 + \theta(h) - 2\underline{\theta_r}) K(h) dh} \\
 &= \lim_{h_0 \rightarrow -\infty} S_{K-V2}(\underline{h_0}, h_1)
 \end{aligned} \tag{12}$$

115

with the specific function S_{K-V2} defined as follows:

$$S_{K-V2}(h_0, h_1) = \sqrt{\int_{h_0}^{h_1} (\theta_1 + \theta(h) - 2\theta_r) K(h) dh} \tag{13}$$



In comparison to S_K , the water content θ_0 is replaced with θ_r in the integrand for S_{K-V2} . We expect this modification to improve numerical convergence towards the lower integration limit, since S_{K-V2} directly integrates the right integrand (Fig. 2a, S_{K-V2}). Conversely, S_K integrates a distinct integrand, i.e., $(\theta_1 + \theta(h) - 2\theta_0) K(h) \neq (\theta_1 + \theta(h) - 2\theta_r) K(h)$, thus involving an additional source of error (Fig. 2a). Briefly, S_K combines the error due to the integral bound $h_0 > -\infty$ and the difference between its integrand and the targeted integrand. Note that the function S_{K-V2} should be restricted to the evaluation of $S(-\infty, h_1)$ and never used for the computation of other cases, i.e., $S(h_0 \neq -\infty, h_1)$, since the water content in the integrand is fixed at θ_r , which corresponds exclusively to the case of $h_0 = +\infty$.

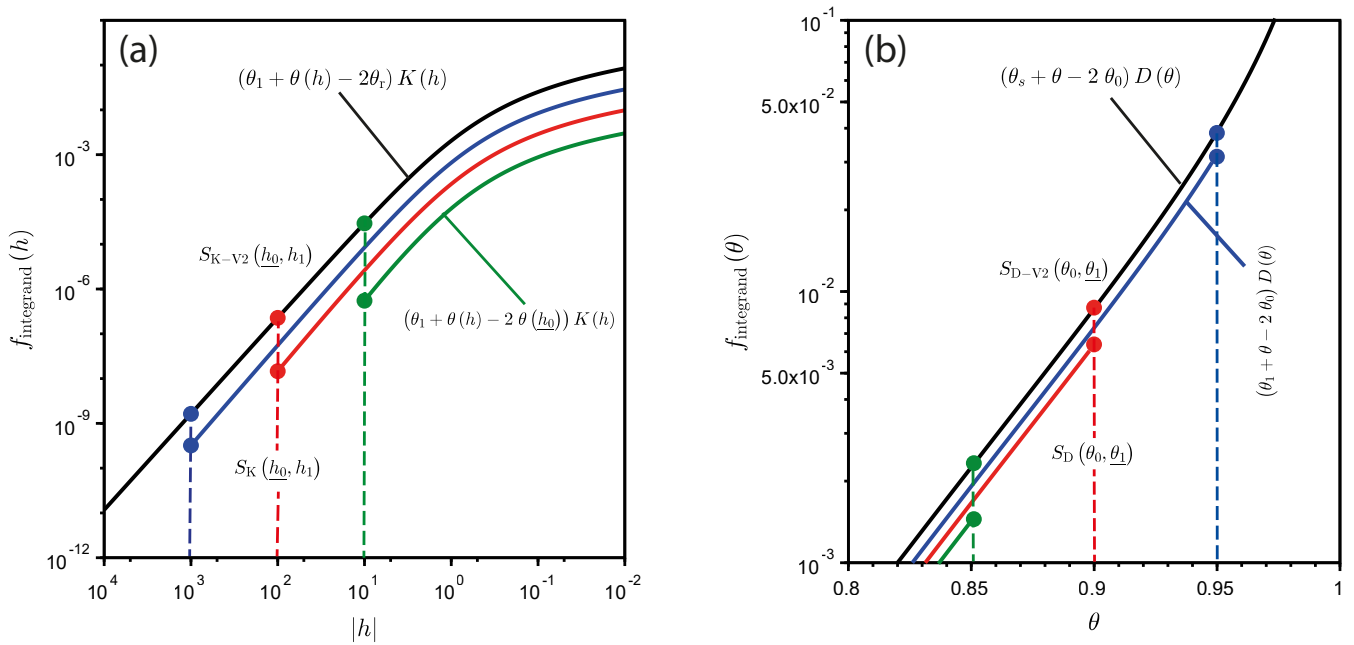


Figure 2. Illustration of the regular strategies for the estimation of the limits: (a) case of very dry conditions with the estimation of $S(-\infty, h_1)$ using either $S_K(h_0, h_1)$ or $S_{K-V2}(h_0, h_1)$, (b) case of saturation $\theta_1 \rightarrow \theta_s$, with the estimation of $S_u(\theta_0, \theta_s)$ using either $S_D(\theta_0, \theta_1)$ or $S_{D-V2}(\theta_0, \theta_1)$. The variables that are varied to reach the targeted limits are underlined. The integration proceeds from the given value of h_0 to right, $h \geq h_0$ in (a) and from the given value of θ_1 to the left, $\theta \leq \theta_1$ in (b), and figures are zoomed in the vicinity of the limits.

125 The application of the scaling, Eqs. (6-7), to the preceding definitions, Eqs. (11-12), leads to scaled versions of those equations, which will be used in the computations below:

$$\begin{aligned}
 S^*(-\infty, h_1^*) &= \lim_{h_0^* \rightarrow -\infty} \int_{h_0^*}^{h_1^*} \left(S_{e,1} + S_e(h^*) - 2 S_e(h_0^*) \right) K_r(h^*) dh^* \\
 &= \lim_{h_0^* \rightarrow -\infty} S_K^*(h_0^*, h_1^*)
 \end{aligned} \tag{14}$$



$$\begin{aligned}
 S^* (-\infty, h_1^*) &= \lim_{h_0^* \rightarrow -\infty} \sqrt{\int_{h_0^*}^{h_1^*} (S_{e,1} + S_e(h^*)) K_r(h^*) dh^*} \\
 &= \lim_{h_0^* \rightarrow -\infty} S_{K-V2}^* (h_0^*, h_1^*)
 \end{aligned} \tag{15}$$

130 with S_K^* and S_{K-V2}^* , the scaled versions of S_K and S_{K-V2} , defined as follows:

$$\begin{cases}
 S_K^* (h_0^*, h_1^*) = \sqrt{\int_{h_0^*}^{h_1^*} (S_{e,1} + S_e(h^*) - 2S_e(h_0^*)) K_r(h^*) dh^*} \\
 S_{K-V2}^* (h_0^*, h_1^*) = \sqrt{\int_{h_0^*}^{h_1^*} (S_{e,1} + S_e(h^*)) K_r(h^*) dh^*}
 \end{cases} \tag{16}$$

The derivation of these equations involved scaling Eq. (6) and Eq. (7) along with the change of variable $\theta \rightarrow S_e$.

2.2.2 Computing sorptivity with S_D for null water pressure head at surface ($h_1 = 0$)

A similar approach is often used with the S_D formulation to avoid numerical indeterminacy close to saturation. The first option
 135 considers $S_D(\theta_0, \theta_1)$ with $\theta_1 \rightarrow \theta_s$ as suggested, for instance, by Fernández-Gálvez et al. (2019):

$$\begin{aligned}
 S_u(\theta_0, \theta_s) &= \sqrt{\int_{\theta_0}^{\theta_s} (\theta_s + \theta - 2\theta_0) D(\theta) d\theta} \\
 &= \lim_{\theta_1 \rightarrow \theta_s} \sqrt{\int_{\theta_0}^{\theta_1} (\theta_1 + \theta - 2\theta_0) D(\theta) d\theta} \\
 &= \lim_{\theta_1 \rightarrow \theta_s} S_D(\theta_0, \theta_1)
 \end{aligned} \tag{17}$$

Note that with this method, we can only account for the unsaturated part of sorptivity, $S_u(\theta_0, \theta_s) = \sqrt{\int_{\theta_0}^{\theta_s} (\theta_s + \theta - 2\theta_0) D(\theta) d\theta}$,
 and we systematically miss the saturated portion of sorptivity $2(\theta_s - \theta_0) K_s(h_1 - h_a)$, as mentioned in section 1. The total
 sorptivity corresponds to the sum of its two components (see Eq. 3): $S(h_0, h_1 > h_a) = \sqrt{S_u^2(\theta_0, \theta_s) + 2(\theta_s - \theta_0) K_s(h_1 - h_a)}$.
 140 The subscript "u" in $S_u(\theta_0, \theta_s)$ stands for "unsaturated" and serves as a reminder of that limitation (Ross et al., 1996). This
 point will be further illustrated and discussed in the Results section (section 3).

The integrand specified by S_D corresponds to $(\theta_1 + \theta(h) - 2\theta_0) D(\theta)$. Consequently, S_D combines the error due to the
 discrepancy between the integrated and the targeted integrands with the error resulting from the restriction of the integration to
 $[\theta_0, \theta_1]$ instead of $[\theta_0, \theta_s]$ (Fig. 2b, S_D). To correct this problem, we define a different estimator, S_{D-V2} , to integrate directly



145 the targeted integrand, $(\theta_s + \theta(h) - 2\theta_0) D(\theta)$ (Fig. 2b, S_{D-V2}), and the following developments come out:

$$\begin{aligned}
 S_u(\theta_0, \theta_s) &= \sqrt{\int_{\theta_0}^{\theta_s} (\theta_s + \theta - 2\theta_0) D(\theta) d\theta} \\
 &= \lim_{\theta_1 \rightarrow \theta_s} \sqrt{\int_{\theta_0}^{\theta_1} (\theta_s + \theta - 2\theta_0) D(\theta) d\theta} \\
 &= \lim_{\theta_1 \rightarrow \theta_s} S_{D-V2}(\theta_0, \theta_1)
 \end{aligned} \tag{18}$$

with the function S_{D-V2} defined as follows:

$$S_{D-V2}(\theta_0, \theta_1) = \sqrt{\int_{\theta_0}^{\theta_1} (\theta_s + \theta - 2\theta_0) D(\theta) d\theta} \tag{19}$$

As mentioned above for S_{K-V2} , S_{D-V2} should be only used for the determination of $S_u(\theta_0, \theta_s)$, and not for the computation
 150 of sorptivity corresponding to other values of final water contents, S_{D-V2} integrates the integrand related exclusively to the case of $\theta_1 = \theta_s$.

The scaled version of these equations can be easily found by applying the scaling, Eq. (6-7), to the previous equations, Eqs. (17-18), leading to their scaled versions:

$$\begin{aligned}
 S_u^*(S_{e,0}, 1) &= \lim_{S_{e,1} \rightarrow 1} \sqrt{\int_{S_{e,0}}^{S_{e,1}} (S_{e,1} + S_e - 2S_{e,0}) D^*(S_e) dS_e} \\
 &= \lim_{S_{e,1} \rightarrow 1} S_D^*(S_{e,0}, S_{e,1})
 \end{aligned} \tag{20}$$

155

$$\begin{aligned}
 S_u^*(S_{e,0}, 1) &= \lim_{S_{e,1} \rightarrow 1} \sqrt{\int_{S_{e,0}}^{S_{e,1}} (1 + S_e - 2S_{e,0}) D^*(S_e) dS_e} \\
 &= \lim_{S_{e,1} \rightarrow 1} S_{D-V2}^*(S_{e,0}, S_{e,1})
 \end{aligned} \tag{21}$$

with the use of the scaled versions S_D^* and S_{D-V2}^* of the formulations S_D and S_{D-V2} :

$$\begin{cases}
 S_D^*(S_{e,0}, S_{e,1}) = \sqrt{\int_{S_{e,0}}^{S_{e,1}} (S_{e,1} + S_e - 2S_{e,0}) D^*(S_e) dS_e} \\
 S_{D-V2}^*(S_{e,0}, S_{e,1}) = \sqrt{\int_{S_{e,0}}^{S_{e,1}} (1 + S_e - 2S_{e,0}) D^*(S_e) dS_e}
 \end{cases} \tag{22}$$

In the following, we compare these previously used strategies based on the use of S_{K^*} , and S_D^* , and the improved versions
 160 designed for the purpose of this study, S_{K-V2}^* and S_{D-V2}^* with the proposed mixed formulation S_M^* , in terms of accuracy



and efficiency. Note that instead of using the limits, some authors (e.g., Minasny and McBratney, 2000) have discretized the integrands using the adaptive Gaussian quadrature algorithm (Kahaner et al., 1989). This point is out of the scope of this study. We focused on regular integration procedures without discretization of integrands and functions, like in the adaptive Gaussian quadrature algorithm (Kahaner et al., 1989).

165 2.3 Validation of estimates against the nominal sorptivity for the selected hydraulic models

2.3.1 Hydraulic models and nominal sorptivity

The validation of the computation of sorptivity with the proposed mixed formulation S_M (Eq. 9) and the usual strategies (see sections 2.2) was performed for hydraulic models that present challenging features. Besides, these models are commonly used for the hydraulic characterization of soils:

- 170 – The Brooks and Corey (BC) model (Brooks and Corey, 1964) is among the first hydraulic models of soil physics (Hillel, 1998). It uses power laws to define the water retention (WR) and hydraulic conductivity (HC) functions and was often considered for integrating sorptivity and finding analytical solutions for water infiltration into soils (e.g., Varado et al., 2006). The **BC model** reads as follows:

$$\begin{cases} \theta_{BC}(h) = \begin{cases} \theta_s & h \geq h_{BC} \\ \theta_r + (\theta_s - \theta_r) \left(\frac{h_{BC}}{h}\right)^{\lambda_{BC}} & h < h_{BC} \end{cases} \\ K_{BC}(\theta) = K_s \left(\frac{\theta - \theta_r}{\theta_s - \theta_r}\right)^{\eta_{BC}} \end{cases} \quad (23)$$

- 175 – The van Genuchten – Burdine (vGB) model combines van Genuchten (1980) model with Burdine condition ($m = 1 - \frac{2}{n}$) for the WR function and the Brooks and Corey (1964) model for the HC function. It was the basis of the development of BEST methods and often considered for the hydraulic characterization of soils (Lassabatere et al., 2006; Yilmaz et al., 2010; Bagarello et al., 2014a). These formulations are considered to be one of the most consistent to use for modeling water infiltration into soils (Fuentes et al., 1992). The **vGB model** reads as follows:

180

$$\begin{cases} \theta_{vGB}(h) = \theta_r + (\theta_s - \theta_r) \left(1 + \left(\frac{h}{h_{vGB}}\right)^{n_{vGB}}\right)^{-m_{vGB}} \\ m_{vGB} = 1 - \frac{2}{n_{vGB}} \\ K_{vGB}(\theta) = K_s \left(\frac{\theta - \theta_r}{\theta_s - \theta_r}\right)^{\eta_{vGB}} \end{cases} \quad (24)$$

- The van Genuchten – Mualem (vGM) model combines van Genuchten (1980) model with Mualem's condition ($m = 1 - \frac{1}{n}$) for the WR function and the Mualem (1976) capillary model for the HC function. The vGM model is among the most widely-used models, in particular for the numerical modeling of flow in the vadose zone (Šimůnek et al., 2003). The **vGM model** reads as follows:

185

$$\begin{cases} \theta_{vGM}(h) = \theta_r + (\theta_s - \theta_r) \left(1 + \left(\frac{h}{h_{vGM}}\right)^{n_{vGM}}\right)^{-m_{vGM}} \\ m_{vGM} = 1 - \frac{1}{n_{vGM}} \\ K_{vGM}(\theta) = K_s \left(\frac{\theta - \theta_r}{\theta_s - \theta_r}\right)^{l_{vGM}} \left(1 - \left(1 - \left(\frac{\theta - \theta_r}{\theta_s - \theta_r}\right)^{\frac{1}{m_{vGM}}}\right)^{m_{vGM}}\right)^2 \end{cases} \quad (25)$$



– The Kosugi (KG) model relates the WR function to the soil pore size distribution assuming log-normal distributions (Kosugi, 1996). It is quite popular as the consequence of its physical meaning and soundness (Pollacco et al., 2013; Nasta et al., 2013) and was also recently implemented into BEST methods for the hydraulic characterization of soils (Fernández-Gálvez et al., 2019). The **KG model** reads as follows:

$$190 \quad \begin{cases} \theta_{KG}(h) = \theta_r + \frac{(\theta_s - \theta_r)}{2} \operatorname{erfc} \left(\frac{\ln \left(\frac{h}{h_{KG}} \right)}{\sqrt{2} \sigma_{KG}} \right) \\ K_{KG}(\theta) = K_s \left(\frac{\theta - \theta_r}{\theta_s - \theta_r} \right)^{l_{KG}} \left(\frac{1}{2} \operatorname{erfc} \left(\operatorname{erfc}^{-1} \left(2 \frac{\theta - \theta_r}{\theta_s - \theta_r} + \frac{\sigma_{KG}}{\sqrt{2}} \right) \right) \right)^2, \end{cases} \quad (26)$$

where erfc stands for the complementary error function.

These models involve the following common scale hydraulic parameters: residual water content, θ_r , saturated water content, θ_s , scale parameter for the water pressure head, h_g , (h_{BC} , h_{vGB} , h_{vGM} , or h_{KG}), and saturated hydraulic conductivity, K_s . The BC models involve a non-null air-entry water pressure head, h_{BC} , meaning that air needs a given suction to enter into the soil and to desaturate the soil. For the sake of simplicity, the scale parameter for water pressure head is often fixed at the air-entry pressure head, so that $h_g = h_{BC}$. In addition, these hydraulic models involve one or two shape parameters for each set of WR and HC functions, which are λ_{BC} and η_{BC} for the BC model, m_{vGB} , n_{vGB} and η_{vGB} for the vGB model, m_{vGM} , n_{vGM} and l_{vGM} for the vGM model, and, lastly, σ_{KG} and l_{KG} for the KG model. In order to simplify these equations and to reduce the risk of equifinality and non-unique optimization when inverting (Pollacco et al., 2013), the following capillary model has been proposed to link these shape parameters (Haverkamp et al., 2005):

$$200 \quad \eta = \frac{2}{\lambda} + 2 + p \quad (27)$$

where $\lambda = \lambda_{BC}$ for the BC model and $\lambda = mn$ for the vGB models. Besides, the shape parameters l_{vGM} and l_{KG} are usually fixed at $\frac{1}{2}$. In this study, the computations are performed considering the relationship given by Eq. (27).

The application of the scaling procedure Eq. (6) to these hydraulic models, i.e., Eqs. (23)-(26) leads to the following scaled hydraulic models (Lassabatere et al., 2021):

BC model:

$$\begin{cases} S_{e,BC}(h^*) = (1 - H(1 + h^*)) |h^*|^{-\lambda_{BC}} + H(1 + h^*) \\ K_{r,BC}(S_e) = S_e^{\eta_{BC}} \end{cases} \quad (28)$$

vGB model:

$$\begin{cases} S_{e,vGB}(h^*) = (1 + |h^*|^{n_{vGB}})^{-m_{vGB}} \\ \text{with } m_{vGB} = 1 - \frac{2}{n_{vGB}} \\ K_{r,vGB}(S_e) = S_e^{\eta_{vGB}} \end{cases} \quad (29)$$

210 **vGM model:**

$$\begin{cases} S_{e,vGM}(h^*) = (1 + |h^*|^{n_{vGM}})^{-m_{vGM}} \\ \text{with } m_{vGM} = 1 - \frac{1}{n_{vGM}} \\ K_{r,vGM}(S_e) = S_e^{l_{vGM}} \left(1 - \left(1 - S_e^{\frac{1}{m_{vGM}}} \right)^{m_{vGM}} \right)^2 \end{cases} \quad (30)$$



KG model:

$$\begin{cases} S_{e,KG}(h^*) = \frac{1}{2} \operatorname{erfc}\left(\frac{\ln(|h^*|)}{\sqrt{2}\sigma_{KG}}\right) \\ K_{r,KG}(S_e) = S_e^{l_{KG}} \left(\frac{1}{2} \operatorname{erfc}\left(\operatorname{erfc}^{-1}(2S_e) + \frac{\sigma_{KG}}{\sqrt{2}}\right)\right)^2. \end{cases} \quad (31)$$

These hydraulic models have the following hydraulic diffusivity functions, $D^*(S_e) = K(S_e) \frac{dh^*}{dS_e}$ (Lassabatere et al., 2021):

$$215 \quad D_{BC}^*(S_e) = \frac{1}{\lambda_{BC}} S_e^{\eta_{BC} - \left(\frac{1}{\lambda_{BC}} + 1\right)} \quad (32)$$

$$D_{vGB}^*(S_e) = \frac{1 - m_{vGB}}{2m_{vGB}} S_e^{\eta_{vGB} - \frac{1+m_{vGB}}{2m_{vGB}}} \left(1 - S_e^{\frac{1}{m_{vGB}}}\right)^{-\frac{1+m_{vGB}}{2}} \quad (33)$$

$$D_{vGM}^*(S_e) = \frac{1 - m_{vGM}}{m_{vGM}} S_e^{l_{vGM} - \frac{1}{m_{vGM}}} \left(\left(1 - S_e^{\frac{1}{m_{vGM}}}\right)^{-m_{vGM}} + \left(1 - S_e^{\frac{1}{m_{vGM}}}\right)^{m_{vGM}} - 2 \right) \quad (34)$$

220

$$D_{KG}^*(S_e) = \frac{1}{2} \sqrt{\frac{\pi}{2}} \sigma_{KG} S_e^{l_{KG}} \left(\operatorname{erfc}\left(\operatorname{erfc}^{-1}(2S_e) + \frac{\sigma_{KG}}{\sqrt{2}}\right) \right)^2 e^{(\operatorname{erfc}^{-1}(2S_e))^2 + \sqrt{2}\sigma_{KG} \operatorname{erfc}^{-1}(2S_e)} \quad (35)$$

These equations are needed for the computation of the dimensionless sorptivity with the proposed mixed formulation S_M^{*2} , and the regular formulations S_K^{*2} , S_{K-V2}^{*2} , S_D^{*2} and S_{D-V2}^{*2} .

The studied hydraulic models exhibit contrasting and challenging features for the computation of sorptivity, including non-
 225 null water pressure heads $h_a^* < 0$, and infinite hydraulic diffusivity close to saturation $\lim_{S_e \rightarrow 1} D^*(S_e) = +\infty$. The complexity may also increase with the values of related shape parameters. To that regards, Lassabatere et al. (2021) define a shape index to characterize the spread of the WR functions around $S_e(h^*) = \frac{1}{2}$. Regardless the chosen hydraulic model, the values of x close to zero correspond to a large spread of WR functions with a smooth descent of the saturation degree, S_e , with the increase of $|h^*|$ (See Fig. 2, in Lassabatere et al. (2021), and also section 3). Conversely, when x gets close to unity, WR functions
 230 approach the stepwise function with an abrupt decrease of S_e with the increase of $|h^*|$. Lassabatere et al. (2021) defined the WR shape index x as follows:

$$\begin{cases} x_{BC} = \frac{\lambda_{BC}}{2 + \lambda_{BC}} \\ x_{vGB} = m_{vGB} \\ x_{vGM} = m_{vGM} \\ x_{KG} = \frac{1}{1 + \sigma_{KG}} \end{cases} \quad (36)$$



Lassabatere et al. (2021) also determined analytically the maximum square scaled sorptivity $S^{*2}(-\infty, 0)$, also referred to as the parameter c_p , as a function of the WR shape index x , for the BC, vBG, and vGM models:

$$\begin{cases}
 c_{p,BC}(x) = 2 + \frac{1-x}{5x+1} + \frac{1-x}{7x+1} \\
 c_{p,vGB}(x) = \Gamma\left(\frac{3-x}{2}\right) \left[\frac{\Gamma\left(\frac{1+5x}{2}\right)}{\Gamma(1+2x)} + \frac{\Gamma\left(\frac{1+7x}{2}\right)}{\Gamma(1+3x)} \right] \\
 c_{p,vGM}(x) = \Gamma(2-x) \left[\frac{\Gamma\left(\frac{3}{2}x\right)}{\left(\frac{3}{2}x-1\right)\Gamma\left(\frac{1}{2}x\right)} + \frac{\Gamma\left(\frac{5}{2}x\right)}{\left(\frac{5}{2}x-1\right)\Gamma\left(\frac{3}{2}x\right)} \right] + (x-1) \left[\frac{\Gamma\left(\frac{3}{2}x\right)\Gamma(1+x)}{\left(\frac{3}{2}x-1\right)\Gamma\left(\frac{5}{2}x\right)} + \frac{\Gamma\left(\frac{5}{2}x\right)\Gamma(1+x)}{\left(\frac{5}{2}x-1\right)\Gamma\left(\frac{7}{2}x\right)} - 2\left(\frac{1}{\frac{3}{2}x-1} + \frac{1}{\frac{5}{2}x-1}\right) \right]
 \end{cases} \quad (37)$$

235

Note that no analytical formulation can be found for the case of Kosugi's hydraulic model, so $c_{p,KG}(x)$ must be computed numerically (Lassabatere et al., 2021). Note also that in Eqs. (37), nominal sorptivities are defined with the use of the capillary model Eq. (27) for the BC and vGB models, and $l_{vGM} = l_{KG} = \frac{1}{2}$.

2.3.2 Paper methodology and computations

240 In this study, we aim to demonstrate the following points: (i) the studied hydraulic models for WR and HC functions exhibit challenging conditions for the computation of sorptivity, (ii) the proposed mixed formulation is an ideal estimator for sorptivity, and (iii) the usual methods, based on the use of S_K and S_D (Eq. 2 and Eq. 1), or their improved version, S_{K-V2} and S_{D-V2} (Eq. 13 and Eq. 19) do not necessarily provide accurate estimations of the targeted nominal sorptivity. To demonstrate these points, we consider the following conditions. Firstly, we only investigate the case of the scaled sorptivity. Indeed, if we let be
 245 any estimator \hat{S} of the nominal dimensional sorptivity S , and the related scaled variables, \hat{S}^* and S^* , the following relations emerge:

$$\begin{aligned}
 E_r(S) &= \frac{\hat{S} - S}{S} \\
 &= \frac{\hat{S}^* \cdot \sqrt{h_g K_s (\theta_s - \theta_r)} - S^* \cdot \sqrt{h_g K_s (\theta_s - \theta_r)}}{S^* \cdot \sqrt{h_g K_s (\theta_s - \theta_r)}} \\
 &= \frac{\hat{S}^* - S^*}{S^*} \\
 &= E_r(S^*),
 \end{aligned} \quad (38)$$

proving that the accuracy of the scaled estimator corresponds exactly to the accuracy of the dimensional estimator. Lastly, we consider the maximum scaled sorptivity $S^*(-\infty, 0)$, since it involves at the same time the two types of challenges, i.e., very
 250 dry initial conditions with infinite water pressure head, $h_0 = -\infty$, and saturated final conditions with null water pressure head, $h_1 = 0$.

The first step, point (i), involves the study of the selected models with regards to the shapes of WR and HC functions. We computed the WR and HC functions for the four selected models, considering the following values of the WR shape index: $x \in \{0.01, 0.02, \dots, 0.99\}$. For the second goal of the study, point (ii), we compared the values provided by the proposed mixed



255 formulation S_M^* with the nominal (error-free) values of sorptivity, $S^* = S^*(-\infty, 0) = \sqrt{c_p}$, provided by the exact analytical
formulations (Eqs. 37) for BC, vGB and vGM models. The computations were performed for all the values of the WR shape
index x , and the accuracy of S_M^* was discussed as a function of x . For the third goal, point (iii), the estimations provided by the
usual strategies were compared to the estimates provided by the proposed mixed formulation, S_M^{*2} , to evaluate the efficiency of
those previously used strategies. We considered several scenarios for the use of S_K , S_{K-V2} , S_D , S_{D-V2} , with several values
260 of the lower water pressure head h_0^* used in Eq. (14) and Eq. (15), and several values of the final saturation degree $S_{e,1}$ used in
Eq. (20) and Eq. (21). All the computations were performed using Scilab software (Campbell et al., 2010).

3 Results

3.1 Analysis of the selected hydraulic models and related challenging features

The BC model has a non-null air-entry water pressure head (Fig. 3a, shown by the plateau for $|h^*| \leq 1$, i.e., $h^* \geq -1$), meaning
265 that the sorptivity has a non-null saturated part that must be accounted for. This condition is one of the challenging features
of the diffusivity form of sorptivity, Eq. (1). Conversely, the three other hydraulic models do not have any air-entry water
pressure head values (Fig. 3e, i, m do not have plateaus), but rather have infinite values of the hydraulic diffusivity close to
saturation, thus posing potential problems of convergence (Fig. 3h, l, p). The use of these models allows us to characterize the
improvements offered by S_M^* compared to the usual use of S_D^* for the cases of problematic computation close to saturation (i.e.,
270 $h_1 \rightarrow 0$ and $\theta_1 \rightarrow \theta_s$). Similarly, accuracy of the commonly used S_K^* version can be challenged when integrating over infinite
intervals $(-\infty, 0]$, particularly for hydraulic models that are characterized by a slow decrease in the saturation degree, S_e , for
quasi-infinite water pressure heads, h^* . The chosen hydraulic models are thus expected to be challenging, in particular the BC,
vGB and vGM models, which keep high values of saturation degrees even for quasi-infinite water pressure heads (Fig. 3a, e,
i). The KG model, which is more symmetrical and characterized by a larger decrease in S_e when h^* decreases (Fig. 3m) is
275 expected to be less challenging. Regarding those challenges, the shapes of the WR, HC and hydraulic diffusivity functions are
also of importance. We expect the small values of x to be more problematic, in particular with the use of S_K^* , due to the smooth
decrease in S_e with h^* (Fig. 3, first column). Conversely, we expect more problems with the use of S_D^* for large values of x ,
with quasi infinite values for the hydraulic diffusivity close to saturation, i.e., $S_e \rightarrow 1$ (Fig. 3h, l, p).

3.2 Validation of the proposed mixed formulation, S_M^* , against the nominal sorptivity, $S^*(-\infty, 0)$

280 The computations using S_M^* (Eq. 9-10) with $h_c^* = h^* \left(\frac{S_{e,0} + S_{e,1}}{2} \right)$ was efficient in most cases, regardless of the value of the
WR shape index x . The use of the threshold 10^z was necessary for the first value of the WR shape index x for the BC
model ($x_{BC} = 0.01$), the first two values for the vGB model ($x_{vGB} \in \{0.01, 0.02\}$) and the first 17 values for the vGM model
($x_{vGM} \in \{0.01, 0.02, \dots, 0.17\}$). The value of $z = 0$ was enough to allow the computation in all cases, apart from the case of
vGM model for which the value of $z = -1$ had to be considered for $x_{vGM} \in \{0.02, \dots, 0.07\}$ and $z = -2$ for $x_{vGM} = 0.01$.
285 Note that, as long as convergence is obtained, the values of $S_M^*(-\infty, 0)$ do not depend on z . With this strategy involving a

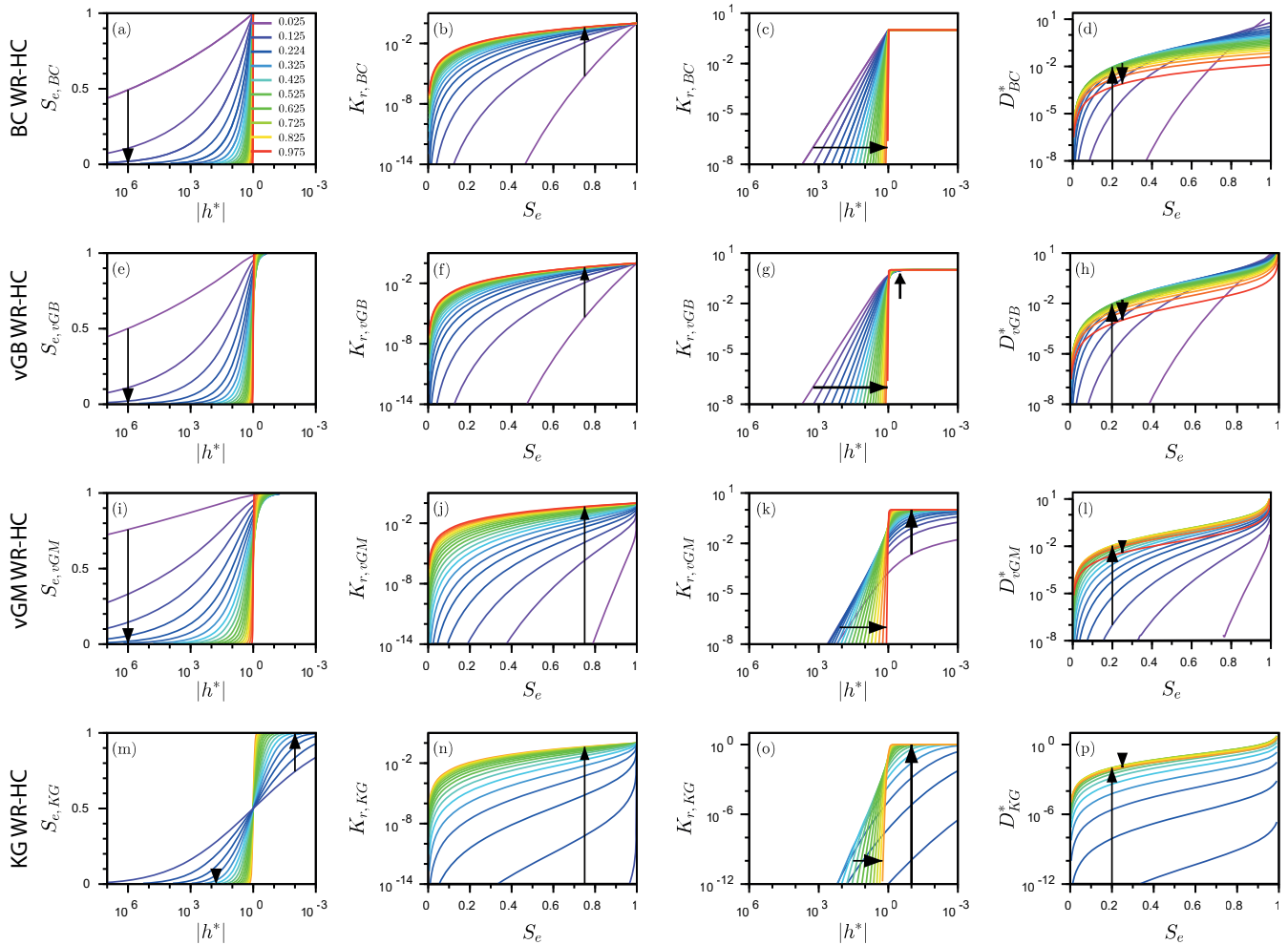


Figure 3. Water retention (WR) and hydraulic conductivity (HC) curves for different values of the WR shape index x . The first column shows WR as $S_e(h^*)$, the second column shows HC as $K_r(S_e)$, the third column shows HC as $K_r(h^*)$, and the fourth column shows diffusivity as $D^*(S_e)$; the four tested models include Brooks and Corey (BC) (1st row), van Genuchten – Burdine (vGB) (2nd row), van Genuchten-Mualem (vGM) (3rd row), and Kosugi (KG) models (4rd row). The arrows indicate the trends with increasing WR shape index x . The hydraulic parameters λ_{BC} , m_{vGM} , m_{vGB} , and σ_{KG} were computed as a function of x using Eq. (36) with $l_{vGM} = l_{KG} = \frac{1}{2}$. Adapted from Lassabatero et al. (2021).

threshold, the proposed mixed formulation, S_M^* , provides estimates for all cases, i.e., for all hydraulic models and all values of the WR shape index, x . A sensitivity analysis was also performed for the KG model and led to the same success with $z = 0$ regardless of the value of the WR shape index x_{KG} (data not shown).



Table 1. Absolute values of relative errors, $|E_r|$, between the proposed mixed formulation, S_M^* , and the targeted scaled sorptivity, $S^*(-\infty, 0) = \sqrt{c_p}$, with the mean $\overline{|E_r|}$, the standard deviation ($\sigma_{|E_r|}$), the minimum and the maximum values for the three hydraulic models whose sorptivity is analytically tractable: Brooks and Corey (BC), van Genuchten – Burdine (vGB), van Genuchten-Mualem (vGM). Note that 10^{-16} corresponds to the relative precision of numbers in scilab.

$ E_r $	BC	vGB	vGM
$\overline{ E_r }$	$1.445 \cdot 10^{-13}$	$5.594 \cdot 10^{-13}$	$3.309 \cdot 10^{-9}$
$\sigma_{ E_r }$	$2.774 \cdot 10^{-13}$	$1.014 \cdot 10^{-12}$	$1.934 \cdot 10^{-8}$
min	$< 10^{-16}$	$< 10^{-16}$	$8.255 \cdot 10^{-16}$
max	$1.201 \cdot 10^{-12}$	$6.037 \cdot 10^{-12}$	$2.000 \cdot 10^{-7}$

Relative error, E_r , between the estimates provided by the proposed mixed formulation, $S_M^*(-\infty, 0)$, and the targeted sorptivity, $S^*(-\infty, 0) = \sqrt{c_p}$, were analyzed in terms of means, standard deviations, and minimum and maximum values (Table 1):

$$E_r = \frac{S_M^*(-\infty, 0) - \sqrt{c_p}}{\sqrt{c_p}} \quad (39)$$

The accuracy of the proposed mixed formulation, S_M^* , Eqs. (9-10), is excellent for all the models and all values of WR shape index x (Table 1). The average relative errors were in the order of 10^{-13} for the BC and vGB models, and in the order of 10^{-9} for the vGM model (Table 1, $\overline{|E_r|}$). The minimum errors were $< 10^{-15}$ for all the models (Table 1, min). The maximum errors were $\approx 10^{-12}$ for the BC and the vGB models and $\approx 10^{-7}$ for the vGM model (Table 1, max). In other words, the mixed formulation, S_M^* , provides extremely accurate estimations of the targeted scaled sorptivity $S^*(-\infty, 0)$. The proposed mixed formulation, S_M^* , can therefore be considered to be an excellent estimator of sorptivity in all cases, regardless the choice of the hydraulic model and related values of shape parameters.

3.3 Study of the usual strategies for estimating the nominal sorptivity, $S^*(-\infty, 0)$

In this section, we compare the estimates provided by the strategies commonly considered (i.e., Eqs. (1-2), S_D^* , $S_{D-V_2}^*$, S_K^* and $S_{K-V_2}^*$) with the reference values of the targeted sorptivity $S^* = S^*(-\infty, 0)$. For these comparisons, we consider the analytical formulations of Eq. (37) for the BC, vGB, and vGM models and use the proposed mixed formulation S_M^* for the KG model. Indeed, no analytical expressions are available for this last model, whereas the estimates provided by $S^* = S_M^*$ are very convincing for the BC, vGB, and vGM models (see Section 3.2) and thus S_M^* is assumed to be as accurate for the KG model.

3.3.1 Illustrative example

Firstly, we investigate the accuracy of the limits of the functions S_K^* and $S_{K-V_2}^*$ towards S^* . These functions, in particular S_K^* , are often used without special attention regarding their accuracy. S_K^* and $S_{K-V_2}^*$ converge to the limit S^* when $|h_0^*|$ becomes large enough (Fig. 4, left column). For instance, for the BC model with $\lambda = 0.56$, the use of S_K^* with $h_0^* = -10$ and $h_0^* = -100$



310 has respective relative errors of $E_r = -4.1\%$ and $E_r = -15\%$ (Figure 4a, red dashed line). The second estimator, S_{K-V2}^* ,
converges much faster than S_K^* . With the same values of h_0^* , the relative errors drop below 0.01% in absolute value (Figure 4a,
blue continuous line). In this case, the convergence towards the target can be achieved by integrating from $h_0^* = -10$, with
high accuracy. Such an improvement results from setting the initial saturation degree, $S_{e,0}$, at its target value, $S_{e,0} = 0$, in the
integrand (see Eq. 15 versus Eq. 14). The same conclusions can be stated regardless of the selected hydraulic models (Figure 4c,
315 e, g).

The convergence of the two functions, S_D^* and S_{D-V2}^* , are depicted for the case of BC functions in Figure 4b. For both
estimators, the estimates are far from the target values, S^* , with $|E_r|$ close to 50% . This large error results from the omission
of the saturated part of sorptivity, as explained above (Section 2.2). By design, S_D^* and S_{D-V2}^* converge towards the unsatu-
rated part of sorptivity, $S_u(0,1) = \sqrt{\int_0^1 (1+S_e) D^*(S_e) dS_e}$, and miss the additional saturated part of the scaled sorptivity,
320 $2(S_{e,1} - S_{e,0}) K_r(S_{e,1}) (h_1^* - h_a^*) = 2$, given that $h_1^* = 0$ ($S_{e,1} = 1$), $h_0^* = -\infty$ ($S_{e,0} = 0$), and $h_a^* = 1$. When the saturated
portion is added to the estimators, the convergence becomes excellent (Figure 4b, green line). These results show that the
computation of sorptivity using the integration with regards to saturation degree, like Eq. (1) and Eq. (22), leads to erroneous
estimations. Accounting for the term $2(\theta_s - \theta_0) K_s |h_a|$ in Eq. (3) is thus essential. Note that Eq. (1) is often considered and
used in most studies, even though it can lead to large under-estimation of sorptivity for the case of non-null air-entry water
325 pressure heads. That factor is of prime importance regarding the accurate estimation of sorptivity.

For the other hydraulic models, the estimators S_D^* and S_{D-V2}^* are significantly better (Figure 4d, f, h). Indeed, the air-entry
water pressure head is null in these models, which removes the large underestimation due to the omission of the saturated part
of sorptivity, as observed for BC model. However, the under-estimation remains substantial, with relative errors on the order of
 $15 - 20\%$ for $S_{e,1} = 0.99$ (Figure 4d, f, h). Even when $S_{e,1} = 0.999$, the relative errors are larger than 10% . From these results,
330 we conclude that the determination of the sorptivity, S^* , by approaching the final saturation degree to unity does not provide
good estimates, regardless of the estimators considered. These poor estimates result from the fact that the diffusivity, and thus
the integrand, are infinite. The convergence of the integrals defined by Eqs. (22) and thus Eq. (1) are slow and prevent accurate
estimations. Conversely to the case of S_K^* and S_{K-V2}^* , changing the integrand by fixing it to the targeted integrand does not
significantly improve the convergence.

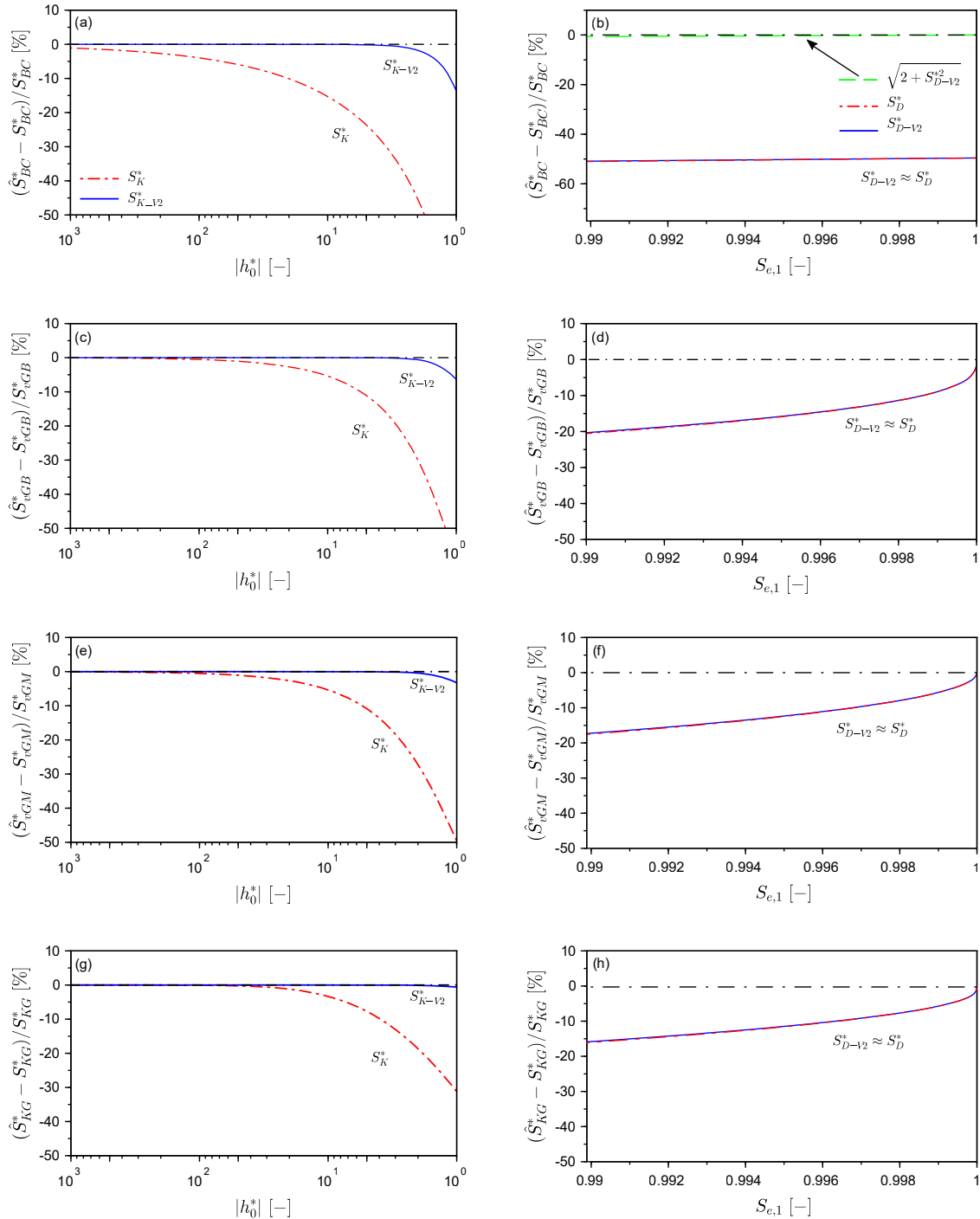


Figure 4. : Relative errors of the regular functions $S_D^*(0, S_{e,1})$ and $S_{D-1/2}^*(0, S_{e,1})$ (right) and $S_K^*(h_0^*, 0)$ and $S_{K-1/2}^*(h_0^*, 0)$ (left) towards $S^*(-\infty, 0)$ for the four hydraulic models, for the following specific cases: BC model with $\lambda_{BC} = 56$ ($x_{BC} = 0.22$), vGB model with $n_{vGB} = 3$ ($x_{vGB} = 1/3$), vGM model with $n_{vGM} = 2$ ($x_{vGM} = 1/2$) with $l_{vGM} = 0.5$, and KG model with $\sigma_{KG} = 1.5$ ($x_{KG} = 0.4$) and $l_{KG} = 0.5$.



335 3.3.2 Relative errors as a function of the WR shape index x

The previous results were presented for specific values of the shape parameters in Figure 4. One may wonder if the accuracy of estimators S_K^* and S_{K-V2}^* , on the one hand, and S_D^* and S_{D-V2}^* , on the other, varies with the shape parameters and indices. Figure 5 depicts the relative errors of the estimators S_K^* and S_{K-V2}^* as a function of the shape parameters for different values of h_0^* (left column of Figure 5) and of the estimators S_D^* and S_{D-V2}^* for different values of $S_{e,1}$ (right column of Figure 5). For all hydraulic models except the BC model, the best estimates for S_D^* and S_{D-V2}^* are obtained for intermediate values of WR shape indexes (Figure 5, right column). Discrepancies increase for both small or large values of the WR shape index. As detailed above (section 3.3.1), accurate predictions require the practitioner to fix the upper integration boundary, $S_{e,1}$, to 0.999 at least, to get errors less than 10%. However, estimates remain poor, even with $S_{e,1} = 0.999$ or $S_{e,1} = 0.9999$, when the WR shape indices tend towards unity (Figure 5d, f, h). For the BC model, the estimators S_D^* and S_{D-V2}^* provide poor estimates under all circumstances, since they miss the saturated part of sorptivity, as explained above (Figure 5b, $S_D^* \approx S_{D-V2}^*$). Adding the saturated part of sorptivity substantially improves the computation, with very accurate estimations (Figure 5b, $\sqrt{(2 + S_D^{*2})}$). Regarding the estimators S_K^* and S_{K-V2}^* (Figure 5, left column), the estimates improve when the WR shape index converges towards 1. It can be noted that S_{K-V2}^* provide always quite accurate predictions with very small relative errors (Figure 5a, c, e, f).

The results obtained in this study also revealed particular behaviors that are specific to different formulations for computing sorptivity, specifically S_K^* , S_{K-V2}^* , S_D^* , and S_{D-V2}^* . The approaches that compute sorptivity by integration with regards to h^* (i.e., S_K^* and S_{K-V2}^*) have errors that come from the choice of the lower integration boundary h_0^* and from the value of $S_{e,0}$ in the integrand. Solutions that compute sorptivity by integration with regards to S_e (i.e., S_D^* and S_{D-V2}^*) have more error associated with the omission of the saturated part, as well as slow convergence of the integration procedure when dealing with infinite diffusivity values. Among the usual procedures, the use of S_K^* is better than S_D^* , but the use of S_{K-V2}^* remains the best one. Indeed, S_{K-V2}^* does not miss the saturated part of sorptivity and provides much lower discrepancies than the other estimators regardless of the selected hydraulic model (Figure 5). At the same time, the adaptation of the integrand, by fixing the values of the initial saturation degree, $S_{e,0}$, to its final values, substantially improves the quality of the estimator. This formulation thus always provides estimates with $|E_r| < 10\%$, regardless of the selected hydraulic model and the value of shape index. However, these errors are still much larger than those obtained with the mixed formulation, S_M^* . Consequently, the use of the mixed formulation, S_M^* , should be favored as far as possible.

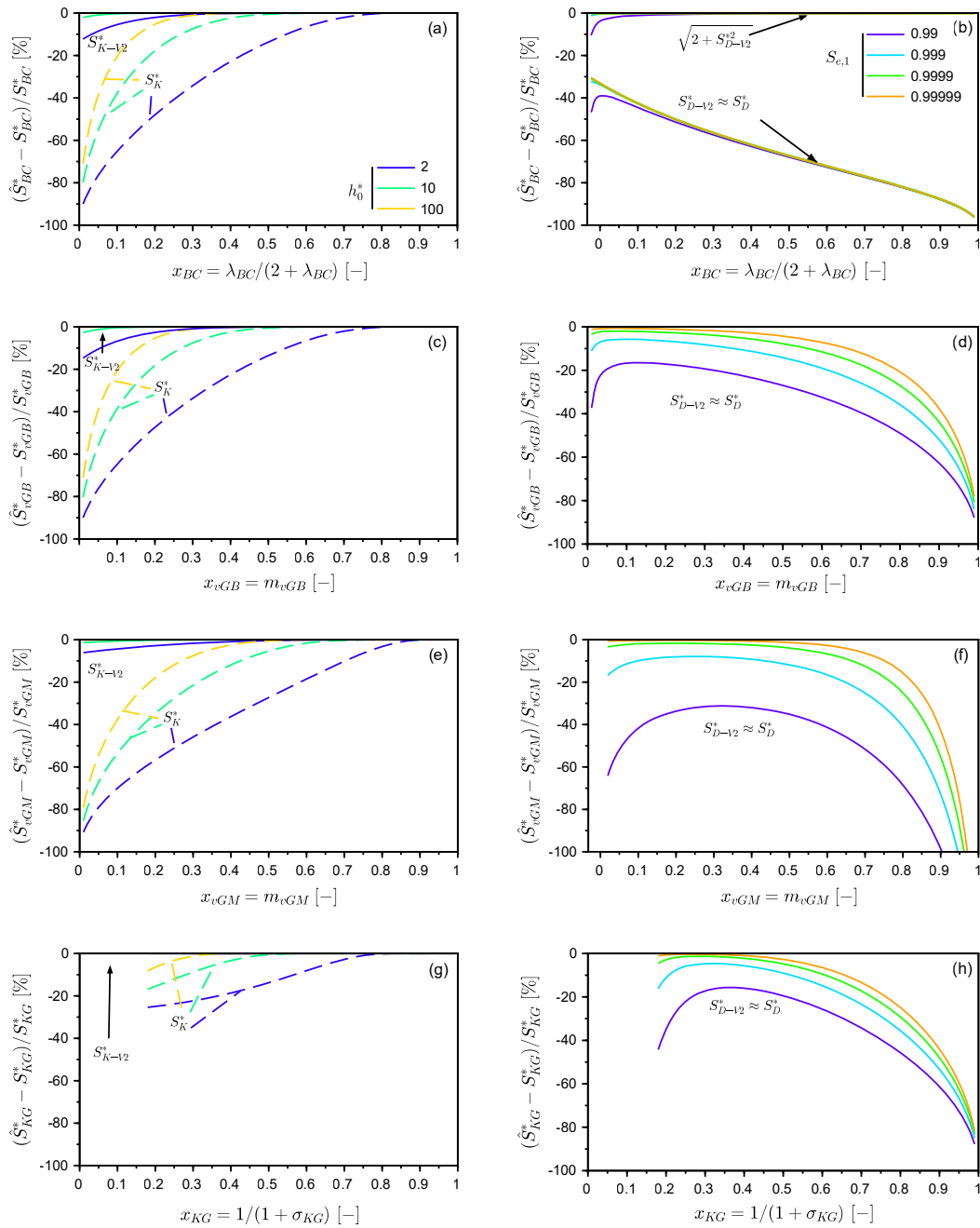


Figure 5. Relative errors of estimators S_D^* and S_{D-V2}^* (right) and S_K^* and S_{K-V2}^* (left) for the four selected hydraulic models, i.e., BC, vGB, vGM, and KG models as a function of the WR shape indexes.



4 Conclusions

The proper evaluation or even calculation of sorptivity is crucial to model accurately water infiltration into soils. However, in some cases, e.g., when the initial state is very dry or the final state corresponds to saturated conditions, the numerical computation of sorptivity using Eq. (1) or Eq. (2) from the hydraulic functions may be a source of numerical errors and difficulties. Indeed, the integration procedure typically used involves either an infinite boundary or unbounded integrands. Many previous studies had attempted to alleviate these problems by fixing arbitrarily finite limits for the integration interval. In this study, we investigated the accuracy of these approaches and demonstrated the potentially massive mis-estimation of sorptivity that is possible when these arbitrary corrections are used. To alleviate those problems, we proposed a mixed formulation that was validated against analytical expressions of sorptivity for specific hydraulic models. The proposed mixed-formulation proved highly accurate for all hydraulic models and shape parameters tested, with negligible relative errors ($< 10^{-7}$).

This study demonstrates that, through the use of the new mixed formulation, it is possible to compute sorptivity easily and very accurately. The proposed formulation presents a very practical tool that may be applied for any type of hydraulic model and any value of initial and final water pressure heads and water contents. The proposed approach allows to compute sorptivity in all cases, thus improving the modeling of water infiltration into soils and the estimation of soil hydraulic properties.

Code availability. Note all computations were done using Scilab free software. The scripts for the computation of all the results and figures presented in this paper, and in particular the script for the proposed mixed formulation can be downloaded online: <https://zenodo.org/record/5789111> (Lassabatere, 2021).

Author contributions. L.L. established the question, performed the analytical developments, computed the numerical results, and provided the first draft of the manuscript. P.-E.P. confirmed the analytical and numerical developments and wrote with L.L. the first draft. D.Y., B.L., D.M.-F., S.d.P. and M.R. verified parts of the numerical computations. J. P. and J. F.-G. helped for the use of the Kosugi model. R.D.S. and M.A.N. helped for the editing, the layout of the manuscript and the presentation of the results. All the authors contributed to the editing of the manuscript.

Competing interests. No competing interest to declare.

Acknowledgements. This work was performed within the INFILTRON project supported by the French National Research Agency (ANR-17-CE04-010).



References

- Angulo-Jaramillo, R., Bagarello, V., Iovino, M., and Lassabatere, L.: Infiltration measurements for soil hydraulic characterization, *Infiltration Measurements for Soil Hydraulic Characterization*, Springer, <https://doi.org/10.1007/978-3-319-31788-5>, 2016.
- 390 Angulo-Jaramillo, R., Bagarello, V., Di Prima, S., Gosset, A., Iovino, M., and Lassabatere, L.: Beerkan Estimation of Soil Transfer parameters (BEST) across soils and scales, *Journal of Hydrology*, 576, 239–261, <https://doi.org/10.1016/j.jhydrol.2019.06.007>, 2019.
- Bagarello, V., Di Prima, S., and Iovino, M.: Comparing alternative algorithms to analyze the beerkan infiltration experiment, *Soil Science Society of America Journal*, 78, 724–736, <https://doi.org/10.2136/sssaj2013.06.0231>, 2014a.
- Bagarello, V., Di Prima, S., Iovino, M., and Provenzano, G.: Estimating field-saturated soil hydraulic conductivity by a simplified Beerkan
395 infiltration experiment, *Hydrological Processes*, 28, 1095–1103, <https://doi.org/10.1002/hyp.9649>, 2014b.
- Bouwer, H.: Unsaturated flow in ground-water hydraulics, *Journal of the Hydraulics Division*, 90, 121–144, <https://doi.org/10.1061/JYCEAJ.0001098>, publisher: American Society of Civil Engineers, 1964.
- Brooks, R. and Corey, A.: *Hydraulic Properties of Porous Media*, Hydrology Papers, Colorado State University, 1964.
- Campbell, S. L., Chancelier, J. P., and Nikoukhah, R.: *Modeling and Simulation in SCILAB*, Modeling and Simulation in Scilab/Scicos with
400 ScicosLab 4.4, 2010.
- Cook, F. and Minasny, B.: Sorptivity of Soils, in: *Encyclopedia of Earth Sciences Series*, pp. 824–826, Springer, https://doi.org/10.1007/978-90-481-3585-1_161, 2011.
- Di Prima, S., Stewart, R., Castellini, M., Bagarello, V., Abou Najm, M., Pirastru, M., Giadrossich, F., Iovino, M., Angulo-Jaramillo, R.,
and Lassabatere, L.: Estimating the macroscopic capillary length from Beerkan infiltration experiments and its impact on saturated soil
405 hydraulic conductivity predictions, *Journal of Hydrology*, 589, <https://doi.org/10.1016/j.jhydrol.2020.125159>, 2020.
- Fernández-Gálvez, J., Pollacco, J., Lassabatere, L., Angulo-Jaramillo, R., and Carrick, S.: A general Beerkan Estimation of Soil Transfer
parameters method predicting hydraulic parameters of any unimodal water retention and hydraulic conductivity curves: Application to the
Kosugi soil hydraulic model without using particle size distribution data, *Advances in Water Resources*, 129, 118–130, 2019.
- Fuentes, C., Haverkamp, R., and Parlange, J.-Y.: Parameter constraints on closed-form soil water relationships, *Journal of hydrology*, 134,
410 117–142, 1992.
- Haverkamp, R., Leij, F. J., Fuentes, C., Sciortino, A., and Ross, P.: Soil water retention, *Soil Science Society of America Journal*, 69,
1881–1890, 2005.
- Hillel, D.: *Environmental soil physics: Fundamentals, applications, and environmental considerations.*, Academic press, 1998.
- Kahaner, D., Moler, C., and Nash, S.: *Numerical methods and software*, Prentice-Hall, Inc., 1989.
- 415 Kosugi, K.: Lognormal Distribution Model for Unsaturated Soil Hydraulic Properties, *Water Resources Research*, 32, 2697–2703,
<https://doi.org/https://doi.org/10.1029/96WR01776>, 1996.
- Lassabatere, L.: Scilab script for mixed formulation for an easy and robust computation of sorptivity,
<https://doi.org/10.5281/zenodo.5789111>, 2021.
- Lassabatere, L., Angulo-Jaramillo, R., Soria Ugalde, J. M., Cuenca, R., Braud, I., and Haverkamp, R.: Beerkan estima-
420 tion of soil transfer parameters through infiltration experiments—BEST, *Soil Science Society of America Journal*, 70, 521,
<https://doi.org/10.2136/sssaj2005.0026>, 2006.
- Lassabatere, L., Angulo-Jaramillo, R., Soria-Ugalde, J., Šimůnek, J., and Haverkamp, R.: Numerical evaluation of a set of analytical infiltra-
tion equations, *Water Resources Research*, 45, <https://doi.org/10.1029/2009WR007941>, 2009.



- Lassabatere, L., Yilmaz, D., Peyrard, X., Peyneau, P., Lenoir, T., Šimůnek, J., and Angulo-Jaramillo, R.: New analytical model for cumulative
425 infiltration into dual-permeability soils, *Vadose Zone Journal*, 13, 1–15, <https://doi.org/10.2136/vzj2013.10.0181>, 2014.
- Lassabatere, L., Di Prima, S., Bouarafa, S., Iovino, M., Bagarello, V., and Angulo-Jaramillo, R.: BEST-2K Method for Characterizing Dual-Permeability Unsaturated Soils with Ponded and Tension Infiltrimeters, *Vadose Zone Journal*, 18, 180–124, <https://doi.org/10.2136/vzj2018.06.0124>, publisher: John Wiley & Sons, Ltd, 2019.
- Lassabatere, L., Peyneau, P.-E., Yilmaz, D., Pollacco, J., Fernández-Gálvez, J., Latorre, B., Moret-Fernández, D., Di Prima, S., Rahmati,
430 M., Stewart, R. D., Abou Najm, M., Hammecker, C., and Angulo-Jaramillo, R.: A scaling procedure for straightforward computation of sorptivity, *Hydrology and Earth System Sciences*, 25, 5083–5104, <https://doi.org/10.5194/hess-25-5083-2021>, 2021.
- Minasny, B. and McBratney, A. B.: Estimation of sorptivity from disc-permeameter measurements, *Geoderma*, 95, 305–324, 2000.
- Mualem, Y.: A new model for predicting the hydraulic conductivity of unsaturated porous media, *Water Resources Research*, 12, 513–522, 1976.
- 435 Nasta, P., Assouline, S., Gates, J. B., Hopmans, J. W., and Romano, N.: Prediction of unsaturated relative hydraulic conductivity from Kosugi’s water retention function, *Procedia Environmental Sciences*, 19, 609–617, 2013.
- Parlange, J.-Y.: On Solving the Flow Equation in Unsaturated Soils by Optimization: Horizontal Infiltration, *Soil Science Society Of America Journal*, 39, 415–418, 1975.
- Pollacco, J., Nasta, P., Soria-Ugalde, J., Angulo-Jaramillo, R., Lassabatere, L., Mohanty, B., and Romano, N.: Reduction
440 of feasible parameter space of the inverted soil hydraulic parameter sets for Kosugi model, *Soil Science*, 178, 267–280, <https://doi.org/10.1097/SS.0b013e3182a2da21>, 27, 2013.
- Ross, P., Haverkamp, R., and Parlange, J.-Y.: Calculating parameters for infiltration equations from soil hydraulic functions, *Transport in porous media*, 24, 315–339, 1996.
- Stewart, R. D. and Abou Najm, M. R.: A comprehensive model for single ring infiltration II: Estimating field-saturated hydraulic conductivity,
445 *Soil Science Society of America Journal*, 82, 558–567, <https://doi.org/10.2136/sssaj2017.09.0313>, 2018.
- van Genuchten, M.: A closed-form equation for predicting the hydraulic conductivity of unsaturated soils., *Soil science society of America journal*, 44, 892–898, 1980.
- Varado, N., Braud, I., Ross, P. J., and Haverkamp, R.: Assessment of an efficient numerical solution of the 1D Richards’ equation on bare soil, *Journal of Hydrology*, 323, 244–257, 2006.
- 450 White, I. and Sully, M. J.: Macroscopic and microscopic capillary length and time scales from field infiltration, *Water Resources Research*, 23, 1514–1522, 1987.
- Yilmaz, D.: Alternative α^* parameter estimation for simplified Beerkan infiltration method to assess soil saturated hydraulic conductivity, *Eurasian Soil Science*, 54, 1049–1058, <https://doi.org/10.1134/S1064229321070140>, 2021.
- Yilmaz, D., Lassabatere, L., Angulo-Jaramillo, R., Deneele, D., and Legret, M.: Hydrodynamic characterization of basic oxygen furnace slag
455 through an adapted best method, *Vadose Zone Journal*, 9, 107–116, <https://doi.org/10.2136/vzj2009.0039>, 2010.
- Šimůnek, J., Jarvis, N. J., van Genuchten, M. T., and Gärdenäs, A.: Review and comparison of models for describing non-equilibrium and preferential flow and transport in the vadose zone, *Journal of Hydrology*, 272, 14–35, 2003.